NYO-9683

BROAD RANGE SPECTROGRAPH

FOR USE WITH THE ROCHESTER 27" CYCLOTRON

by

W. Parker Alford, O. M. Bilaniuk and R. A. Hawrylak

THE UNIVERSITY OF ROCHESTER

DEPARTMENT OF PHYSICS AND ASTRONOMY

ROCHESTER , NEW YORK

AEC DISTRIBUTION LIST

U. S. Atomic Energy Commission (2 copies)
New York Operations Office
Contracts Division
376 Hudson Street
New York 14, New York

U. S. Atomic Energy Commission (1 copy)
Division of Research
Washington 25, D. C.

U. S. Atomic Energy Commission (3 copies)
Office of Technical Information Extension
P. O. Box 62
Oak Ridge, Tennessee

U. S. Atomic Energy Commission (1 copy)
Patents Group
Upton, New York
ATTENTION: Harmon Potter

U. S. Atomic Energy Commission (1 copy)
Washington 25, D. C.
ATTENTION: Roland Anderson

U. S. Atomic Energy Commission (1 copy)
Washington 25, D. C.
ATTENTION: Office of Technical Information

Broad Range Spectrograph for Use with the Rochester 27" Cyclotron*

by

W. Parker Alford, O. M. Bilaniuk and R. A. Hawrylak
Department of Physics and Astronomy
University of Rochester
Rochester, New York

ABSTRACT

A broad range nuclear spectrograph of the Buechner-Bainbridge type, with characteristic radius R = 50 cm has been constructed and installed for use in conjunction with the Rochester 27" variable energy cyclotron. For a given magnetic field, particles are focussed over an energy range $0.6E_o \leq E \leq 1.3E_o$, where E_o is the energy of particles focussed with orbit radius $\rho = R = 50$ cm. The resolution of the spectrograph $\Delta E/E$ is less than 0.2%. Particles may be recorded either in nuclear emulsions or in an array of solid state counters. Results of calibration measurements and typical nuclear data taken with the spectragraph are presented.

---

* Supported by the U. S. Atomic Energy Commission and the Esso Education Foundation. Manufactured to specifications by Spectromagnetic Industries, San Carlos, California.

I. INTRODUCTION

For several years, a large part of the work with the University of Rochester 27" Cyclotron (Fig. 1) has centered on the investigation of nuclear reaction mechanisms and the applicability of various nuclear models to a description of deuteron and proton induced reactions. More recently a gas recovery system has been installed on the vacuum system to allow the use of He^3 in the machine, and work has been started on the study of He^3 induced reactions. Because of the large energy release in most reactions induced by He^3, charged particle spectra from such reactions will generally include protons, deuterons, tritons and alpha particle groups going to many states in the final nucleus, in addition to elastically and inelastically scattered He^3.

For the analysis of such complicated spectra, a new magnetic spectrograph was felt to be necessary. A basic type of design which provided good resolution, reasonable solid angle and focussing over a wide energy range was available in the Buechner-Bainbridge 90^o broad range magnet and the essential optical design for the present magnet was taken from Browne and Buechner. Since it was not expected that the magnet would be used for absolute energy measurements, it was possible to make several

significant simplifications in the mechanical design used by Browne and Buechner, without compromising the requirements for the proposed application. Although the magnet is considerably more compact than Browne and Buechner's, the simplifications do not appear to have affected the qualities of the magnet markedly.

II. DESIGN

The optical properties of the 90^{o} broad range spectrograph are outlined by Browne and Buechner(1) and developed in detail by Braams(2). These may be described briefly by reference to Fig. 2. The focussing field is a uniform field normal to the plane of the figure extending over the shaded portion of the circular area of radius R. Particles from a point source at a distance R from the field boundary enter the field normal to the boundary. Particles of some energy E_o will be deflected through an angle of 90^{o} in an orbit of radius of curvature $\varrho = R$ and will be brought to a vertical line focus at a distance R from the exit field boundary. Particles of different energies will be focussed along a hyperbolic focal surface as indicated in the figure. Theoretical limits for the range of energies focussed are $0.34E_o \leq E \leq 2.9E_o$. At the lower limit particles are focussed at the field

boundary and at the upper limit at infinity. The practical limits on the energy range covered in a given exposure are set mainly by considerations of mechanical designs. In particular, an extension of the energy range much beyond $1.3E_o$ requires an unreasonably large vacuum chamber at the exit of the magnet. Also since the magnet provides only single focussing, the solid angle decreases rather rapidly for energies above E_o.

Original specifications called for a maximum field of 14 kilogauss, with field uniform to within 0.1%. This would allow the magnet to focus protons up to an energy of 33 Mev and deuterons to 16.5 Mev. Thus protons and alphas from any reaction and deuterons from all but two or three possible reactions induced by the cyclotron beam can easily be focussed by the magnet.

By relaxing the original requirements for extremely high field uniformity, a considerable simplification of the Browne-Buechner design was achieved in reducing the magnet yoke structure to a simple C-shape. It was intended to improve the field uniformity, if necessary, by inserting non-magnetic spacers between the pole tips and the yoke, but the uniformity has been found quite satisfactory for present purposes even without the spacers. Another change in the design is the location of the return yoke relative

to the center of curvature of the particle orbits. The available space in the research area dictated that the return yoke be located on the concave side of the particle trajectories. In this case, the stray field in the exit region of the spectrograph is increased but again the actual effect on the performance of the magnet was not significant. Finally, because of the optics of the existing beam analyzer, it was necessary to mount the magnet with the median plane horizontal. In scattering from light nuclei, this introduces appreciable kinematic broadening of peaks as the entrance aperature is opened. The magnet has not yet been used under conditions which would make this a problem. On the other hand the horizontal mounting and the reversed yoke position allow the use of the magnet up to a scattering angle of 165^{o}. Recent measurements of unexpectedly high back-angle cross sections in certain reactions(3) as well as the developments in the distorted-wave-Born-approximation (DWBA) calculations(4) have indicated the importance of measurements at such angles.

III. CONSTRUCTION

The magnet yoke was constructed of USS C1010 low carbon steel. The overall dimensions of the magnet were 3' x 3' x 3' and the weight of the whole structure was about 5 tons. Pole tips, 5" thick, were made of specially heat-treated USS C1010. The faces of the tips were ground flat, and the gap spacing between the tips (3/4") was maintained uniform to within .0001" by a number of brass spacers. In order to minimize scattering of particles inside the pole tips, a series of brass baffles was mounted on each face. The tips formed the top and bottom of the vacuum chamber of the magnet, while the side walls of the chamber were strips of non-magnetic stainless steel welded to the tips. Four ports are provided on the vacuum chamber. At the entrance port a flange carries the adjustable slits which define the beam entering the magnet. On the exit side, the magnet vacuum chamber is extended by a triangular aluminum chamber and a housing at the focal surface for the particle detection system. One of the other ports is located opposite the entrance slit to facilitate alignment of the magnet and the fourth one houses the nuclear magnetic resonance probe.

Two types of detectors have been used with the magnet up to the present. For survey measurements involving many particle groups, nuclear emulsions are used. Three emulsions each 80 x 200 mm can be mounted in a special camera shown in Fig. 3 which allows six different exposures to be made without breaking the spectrograph vacuum. For measurements of a single group, or a few closely spaced groups, a bank of twenty solid state detectors covering a length of 5 cm on the focal surface is used. This system has been described in detail elsewhere(5).

Excitation for the magnet is provided by 128 turns of 1/4" square hollow copper conductor insulated by glass tape and impregnated with epoxy resin. The coils are water cooled, and may easily be run at currents of 400 amperes, the limit of the present power supply.

The magnet is rotated on a horizontal circular rail of 70" diameter, shown in Fig. 2. The axis of rotation for the magnet is provided by a vertical post, 4" in diameter, anchored at the center of the track. The track has been rendered flat and horizontal to within 0.01" by a grinding machine rotated about the vertical post. A 4" thrust bearing, mounted on a shoulder of the post, serves as one of the three points which support the magnet structure. The other two points are the two roller bearing wheels which carry the entire assembly around the center

post. The structure supporting the magnet is assembled out of 6" I-beams and channels assuring adequate rigidity.

Adjustments for vertical, radial, and lateral position of the magnet with respect to the supporting structure are provided. The magnet is moved around the track by a hand crank; gear reducers and the roller bearings make for a smooth and effortless drive. In its motion the magnet carries along the movable components of the continuous rotation scattering chamber(6) which is an integral part of the spectrograph system.

IV. TESTING AND CALIBRATION

Original specifications called for a maximum field of 14 kilogauss, which is easily reached in the magnet. In fact with the existing power supply fields up to 18 kilogauss may be attained. Measurements of field uniformity over the area of the orbits were carried out at fields of 6.8 and 14 kilogauss. For these measurements, a coil of several thousand turns was used as a search coil in conjunction with a Pye fluxmeter. Field variations of 1 gauss could be readily measured. Some non-uniformities up to a few tenths of one percent were found, which were rather larger than expected. However, the location and magnitude of these non-uniformities were the same at both 6.8 and 14 kilogauss, and it was not expected that

these variations would have any significant effect on magnet performance in the intended application. In use the field is measured by a nuclear resonance probe up to fields of 14 kg. At higher fields the signal becomes very poor, indicating that field inhomogenities become more severe as the magnet approaches saturation.

With the magnetic field measured by the nuclear resonance probe, the calibration of the magnet requires a determination of the relationship between the radius of curvature of particle orbits in the uniform field and the position at which the particles are recorded on the focal surface. This relationship was established using alpha particles from a Po^{210} source.[7] The source 1 mm wide x 5 mm high was mounted in the scattering chamber at the object position of the magnet, and the alpha particles focussed through the magnet for a number of different values of the magnetic field. The "spectrum" of Fig. 4 was obtained by recording the alpha group in nuclear emulsions for a fixed time at each field setting. The width of each peak is only slightly greater than would be expected for a source 1 mm in width. The additional width probably arises from the source thickness which was estimated to correspond to a maximum energy loss of 10 kev for the polonium alpha particles. As a matter of convenience, the location of

each peak was taken to be the intercept with the base line of a line drawn through the straight portion of the high energy side of the peak. From the measured positions of the peaks, the relationship between radius of curvature and focal position was obtained, as shown in Fig. 5. Since all exposures were for equal times, the measured intensity of each group provided a measurement of relative solid angle as a function of focal position. This is shown in Fig. 4. The dispersion and magnification of the magnet were not measured systematically, but were checked at a few points, and found to be in satisfactory agreement with calculated values.

A number of curves have been prepared to facilitate the use of the calibration curve, Fig. 5, in determining particle energies. A typical curve is shown in Fig. 6. Here the product $\nu\rho$ (nuclear magnetic resonance frequency times radius of curvature in that field) is plotted versus particle energy for protons. The two curves in the figure refer to the nucleus used in the resonance probe, which may be either hydrogen or lithium. For further convenience in choosing conditions for an exposure, or for rapid identification of rather well separated groups, the information of Figs. 5 and 6 can be combined into a nomograph such as the one shown in Fig. 7. In this nomogram corresponding values of proton energy, lithium resonance frequency

and image position on the focal surface are connected by a straight line.

As an additional aid in the identification of particle groups, a program has been set up to calculate reaction kinematics with the IBM650, and extensive tabulations of kinematics have been prepared for a wide range of reactions on light nuclei.

V. EXAMPLES OF DATA

Examples of spectra taken with the spectrograph on nuclear emulsions are shown in Figures 8 and 9. Data taken with the solid-state counter array have been reported elsewhere (5, 8). The $B^{10}(d,p)B^{11}$ spectrum of Fig. 8 is a composite of three overlapping exposures and covers over 10 Mev of proton energies. The sizes of proton peaks were corrected for the solid angle effect using Fig. 4 so that their relative sizes reflect the relative differential cross sections. It should be noted that the 9.19 - 9.28 Mev doublet in B^{11} is completely resolved. The spectrum of Fig. 9 was obtained in a single exposure in a test run with a self supporting carbon target enriched to 55% in C^{13}. The spectrum covers 50 cm of the image surface (2/3 of the available span) and the range of proton energies recorded is 5 Mev. The 5.28 - 5.31 Mev doublet (30 kev) is only partially resolved, but most of the peak width is accounted

for by beam spread and target thickness.

Fig. 10 shows angular distributions corresponding to the 8.93 Mev, 9.19 Mev and 9.28 Mev states in B^{11} reached via $B^{10}(d,p)B^{11}$ (see Fig. 8) at bombarding energies E_d = 3.4 Mev, 3.8 Mev and 4.0 Mev. The interest of this experiment centers on the parity of the 8.93 Mev state. At E_d = 7.8 Mev and E_d = 8.0 Mev the angular distributions corresponding to this state show very sharp and prominent forward peaking (9) and can be fitted reasonably well with a composite of $\ell = 0$ and $\ell = 2$ Butler curves. This seemed to imply a mixed 2s-1d configuration and even parity for this state. The same reaction at a higher energy, E_d = 10.1 Mev (10) and at lower energies of E_d = 3.0 Mev and 3.5 Mev (11) leads to pure $\ell = 1$ stripping curves thus indicating odd parity for this state. Odd parity for this state is also suggested by Middleton's work on the $B^9(He^3,p)B^{11}$ reaction (12). The data of Fig. 10 were taken as a further check on the angular distribution in question. The results indicate a clear-cut $\ell = 1$ stripping, favoring the odd parity for the 8.93 Mev state. However, the data for the 8.93 Mev state at the bombarding energy of 7.8 Mev were taken simultaneously, and on the same emulsion plates, as the data for the 9.19 Mev and 9.28

Mev states, the latter both showing pure $\ell = 0$ stripping in complete agreement with the distributions at 3.0 Mev, 3.5 Mev (10), 3.4 Mev, 3.8 Mev, 4.0 Mev (present measurement) and 10.1 Mev (10). Since the angular distribution for the 8.93 Mev state at $E_d = 7.8$ Mev was thus monitored by the neighboring groups, which are not in question, it is concluded that the forward peaking observed at $E_d = 7.8$ Mev is real, although it contrasts with similar data at other energies. It is known that patterns of angular distributions calculated with DWBA theory are often very sensitive to the distorting potentials (13). It should prove interesting to see if such calculations will explain the unusual shape of the $B^{10}(d,p)B^{11}$ angular distributions near $E_d = 8$ Mev.

VI. ACKNOWLEDGMENTS

A large number of people have contributed directly or indirectly to the final installation of this magnet. We would particularly like to thank Mr. Donald Klein of Spectromagnetic Industries for his cooperation in the design and construction of the magnet, Mr. Arthur Hamann for his assistance in the electrical installations, and Mr. Michael Armstrong for extensive calculations in connection with the magnet calibration.

REFERENCES

1. C. P. Browne and W. W. Buechner, Rev. Sci. Instr. 27, 904 (1956).

2. C. M. Braams: "Energy Levels in Calcium Isotopes", Ph.D. Thesis, University of Utrecht (1956).

3. O. M. Bilaniuk and W. Parker Alford (to be reported at the Annual Meeting of the APS, January 1962); S. S. M. Wong and E. Bleuler (to be published in Phys. Rev.).

4. W. Tobocman, "Proceedings of the International Conference on Nuclear Structure", p. 307, University of Toronto Press, 1960; R. Satchler, private communication.

5. O. M. Bilaniuk, B. B. Marsh, A. K. Hamann and J. C. Heurtley, Nuclear Instr. and Methods 13, (1961).

6. J. Verba and R. Hawrylak, Rev. Sci. Instr. 32, 1037 (1961).

7. Prepared by the Alpha Laboratory of the AEC Project, University of Rochester, Rochester, New York.

8. W. Parker Alford, O. M. Bilaniuk, and B. B. Marsh, Proceedings of the Rutherford Jubilee International Conference, The University of Manchester, 1961.

9. O. M. Bilaniuk and J. C. Hensel, Phys. Rev. 120, 211 (1960).

10. S. Hinds and R. Middleton, Proceedings of the Rutherford Jubilee International Conference, The University of Manchester, 1961.

11. Work of Pullen and Whitehead, as reported by D. H. Wilkinson, Proceedings of the International Conference on Nuclear Structure, Kingston, Ontario, p. 40, University of Toronto Press, 1960.

12. S. Hinds and R. Middleton, Proc. Phys. Soc. 75, 754 (1960).

13. D. J. Pullen, D. H. Wilkinson, and A. B. Whitehead, Proceedings of the Rutherford Jubilee International Conference, The University of Manchester, 1961.

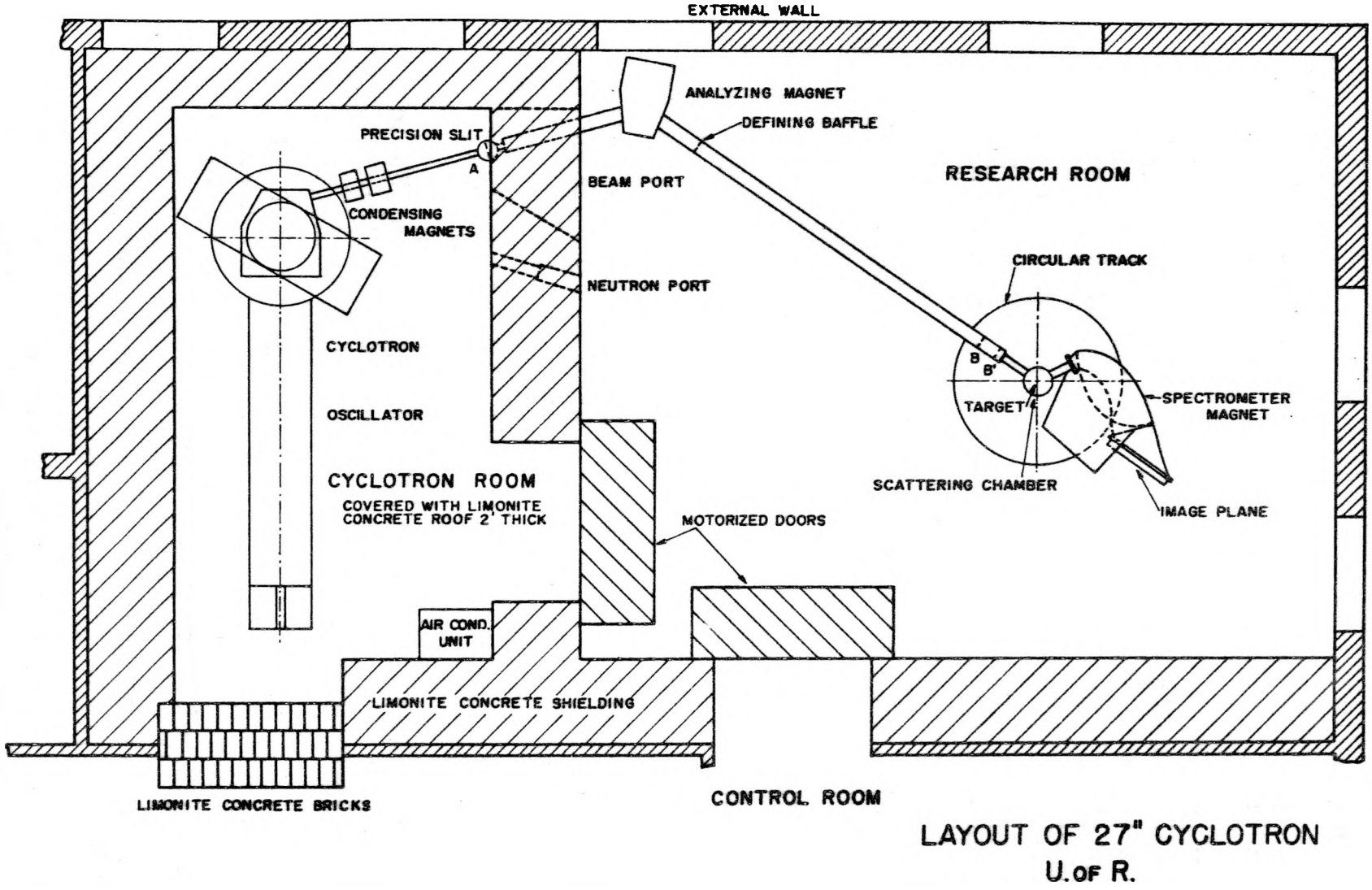

Fig. 1 Layout of the Rochester 27" variable energy cyclotron. The broad range spectrograph is located in the center of the research room. The horizontal mounting and the location of the return yoke on the concave side of the particle trajectories allow the use of the magnet up to a scattering angle of 165°.

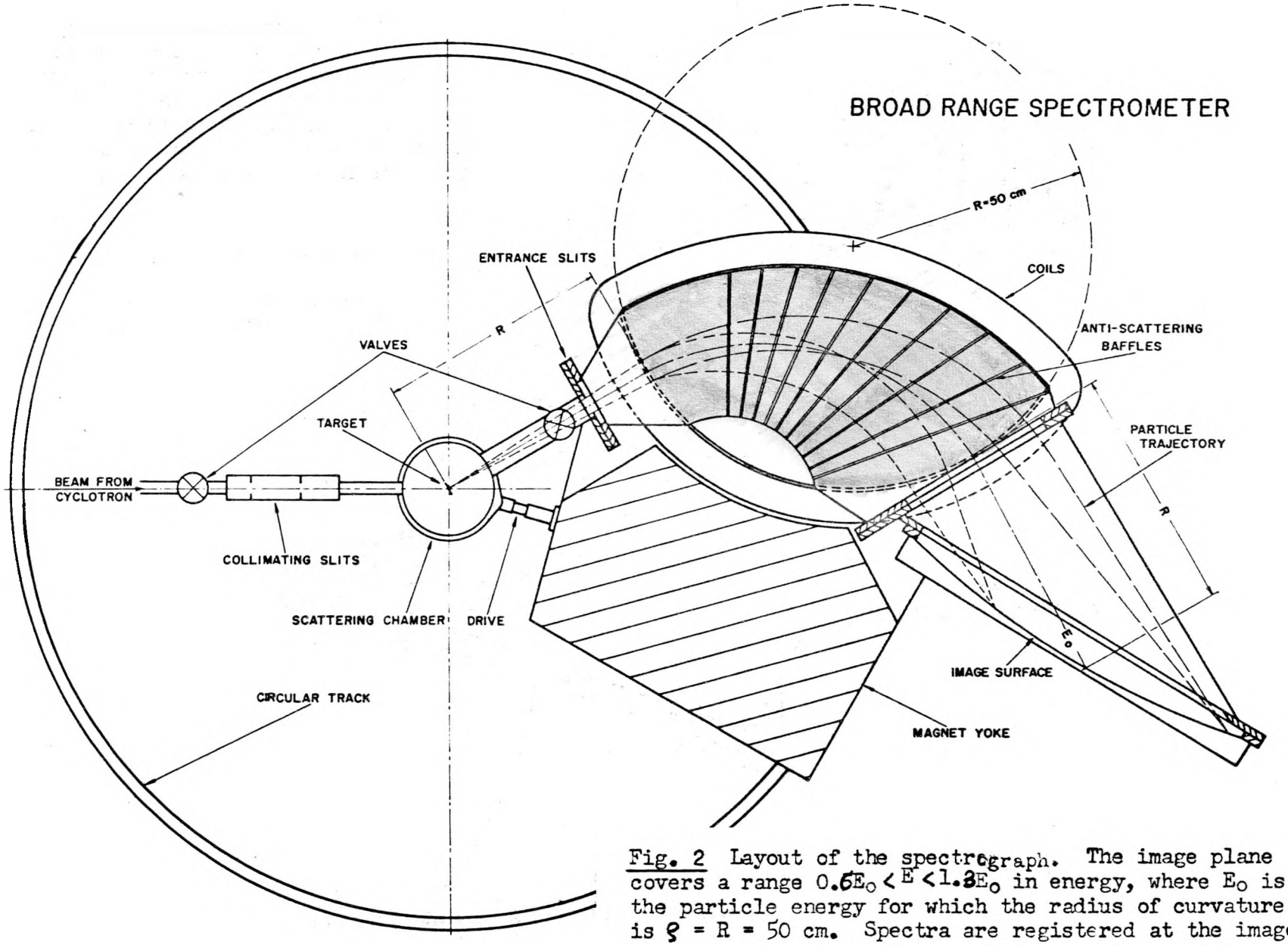

Fig. 2 Layout of the spectrograph. The image plane covers a range $0.6E_0 < E < 1.3E_0$ in energy, where E_0 is the particle energy for which the radius of curvature is $\rho = R = 50$ cm. Spectra are registered at the image surface either in nuclear emulsions or in a solid state counter array.

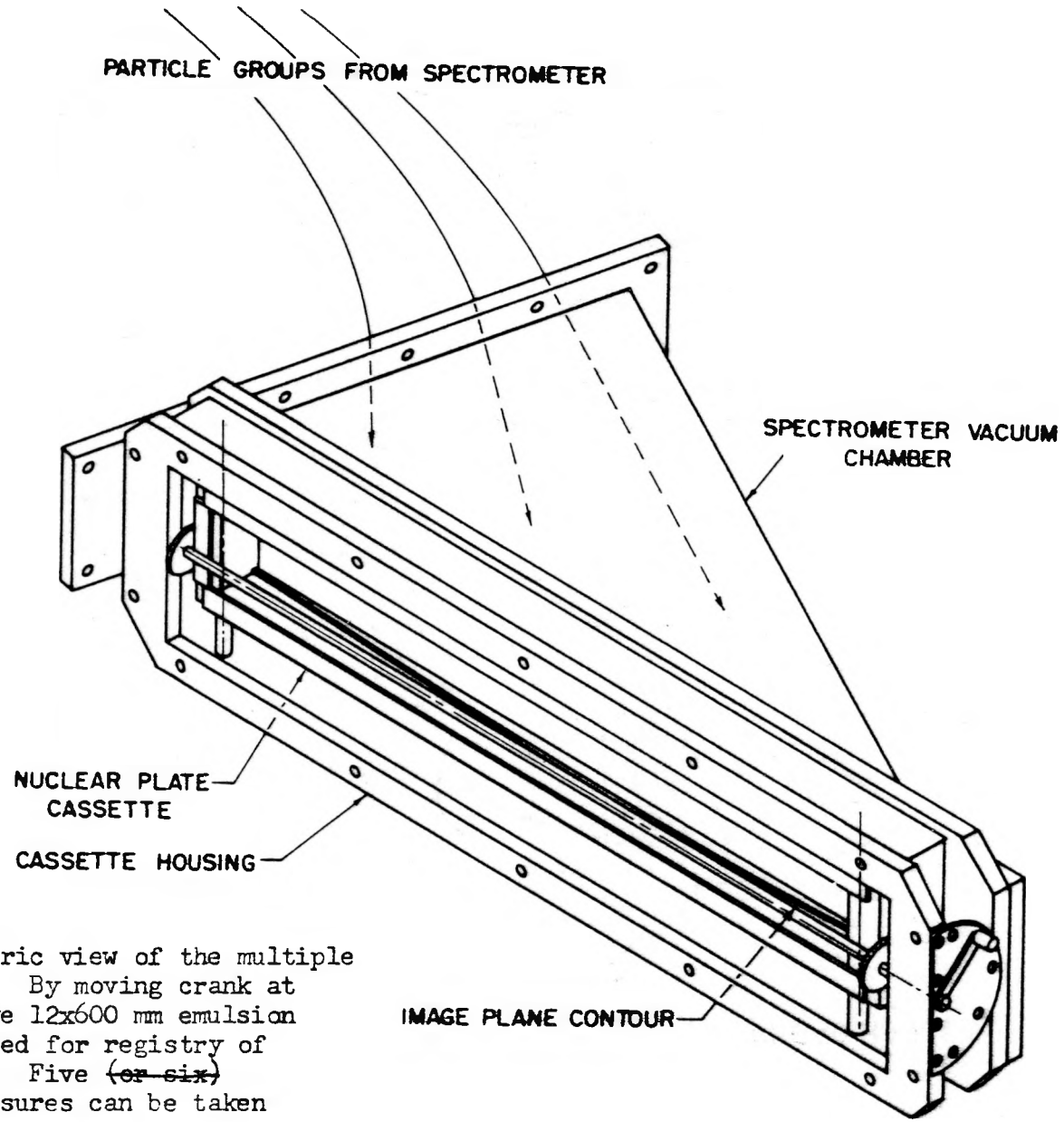

Fig. 3. Isometric view of the multiple exposure camera. By moving crank at right, successive 12x600 mm emulsion strips are exposed for registry of particle groups. Five ~~(or six)~~ independent exposures can be taken without breach of vacuum.

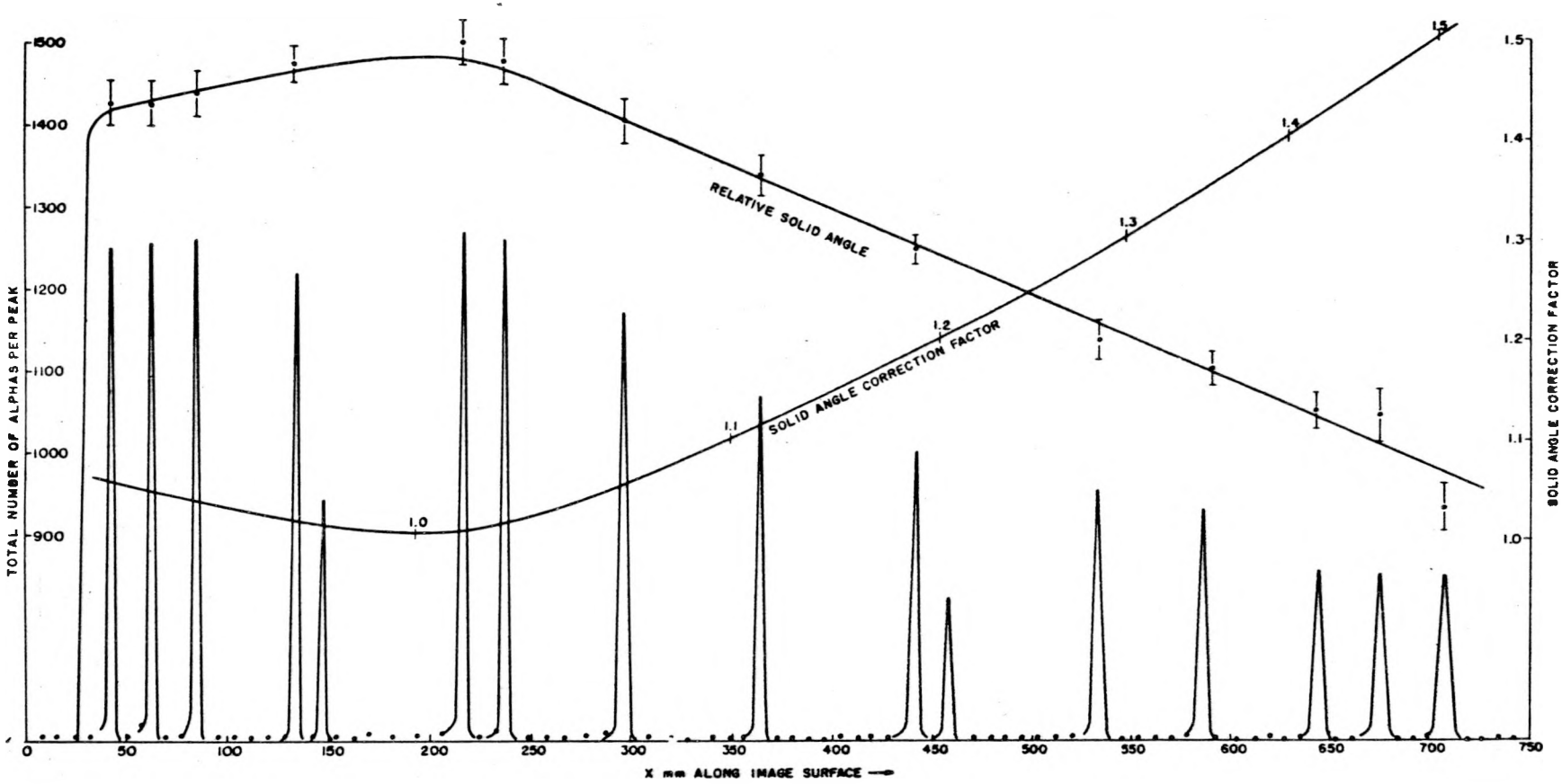

Fig.4. Po^{210} 5.3 Mev alpha groups recorded in nuclear emulsion at different field settings. The groups were recorded for 2 minutes each, except for groups at x = 145 mm and x = 456mm which were taken in one minute each to provide for positive identification of the groups in relation to the magnetic field. The first curve represents the relative solid angle vs. image position as deduced from the total number of alphas per peak. The corresponding correction factor is given by the other curve.

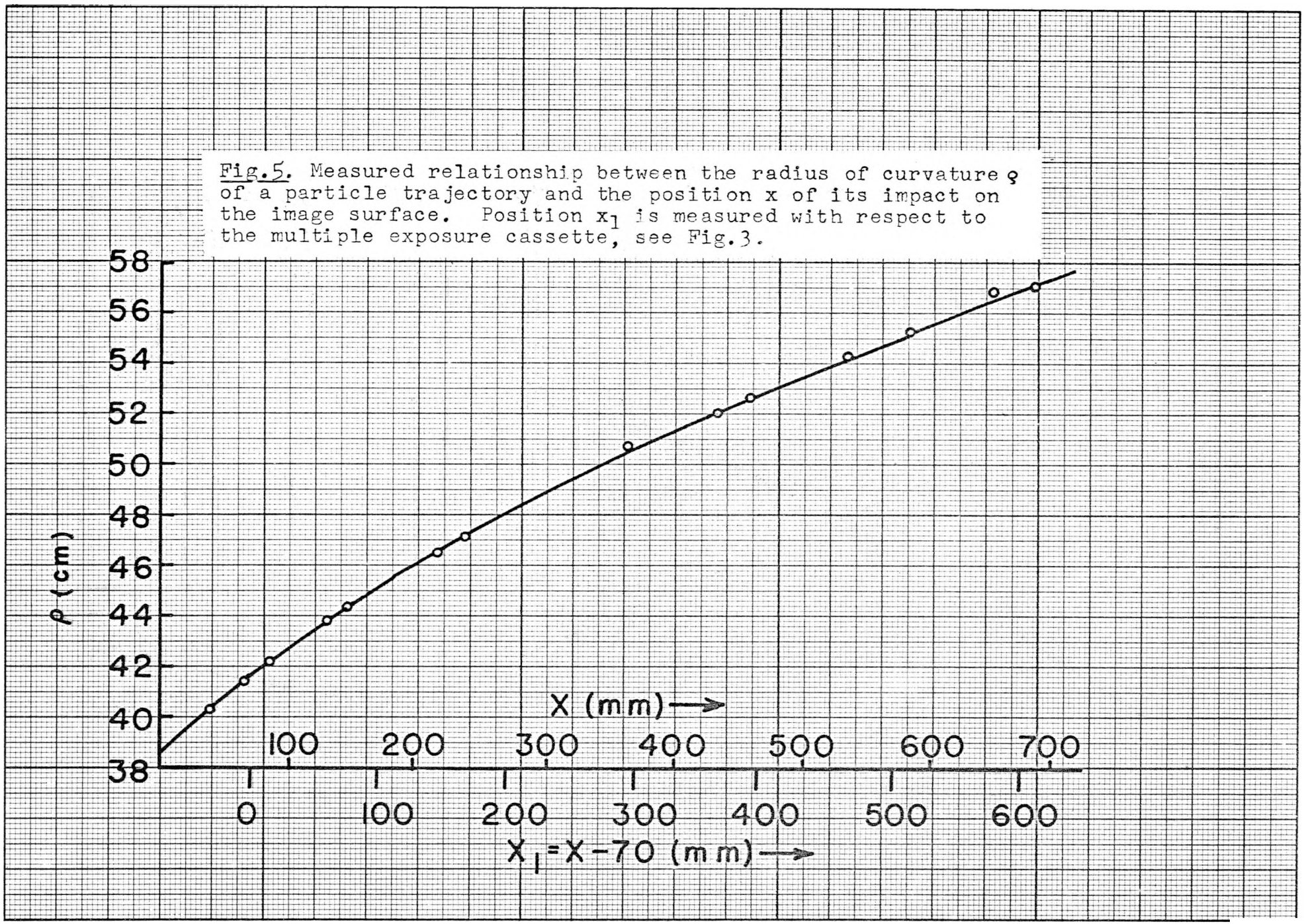

Fig.5. Measured relationship between the radius of curvature ρ of a particle trajectory and the position x of its impact on the image surface. Position x_1 is measured with respect to the multiple exposure cassette, see Fig.3.

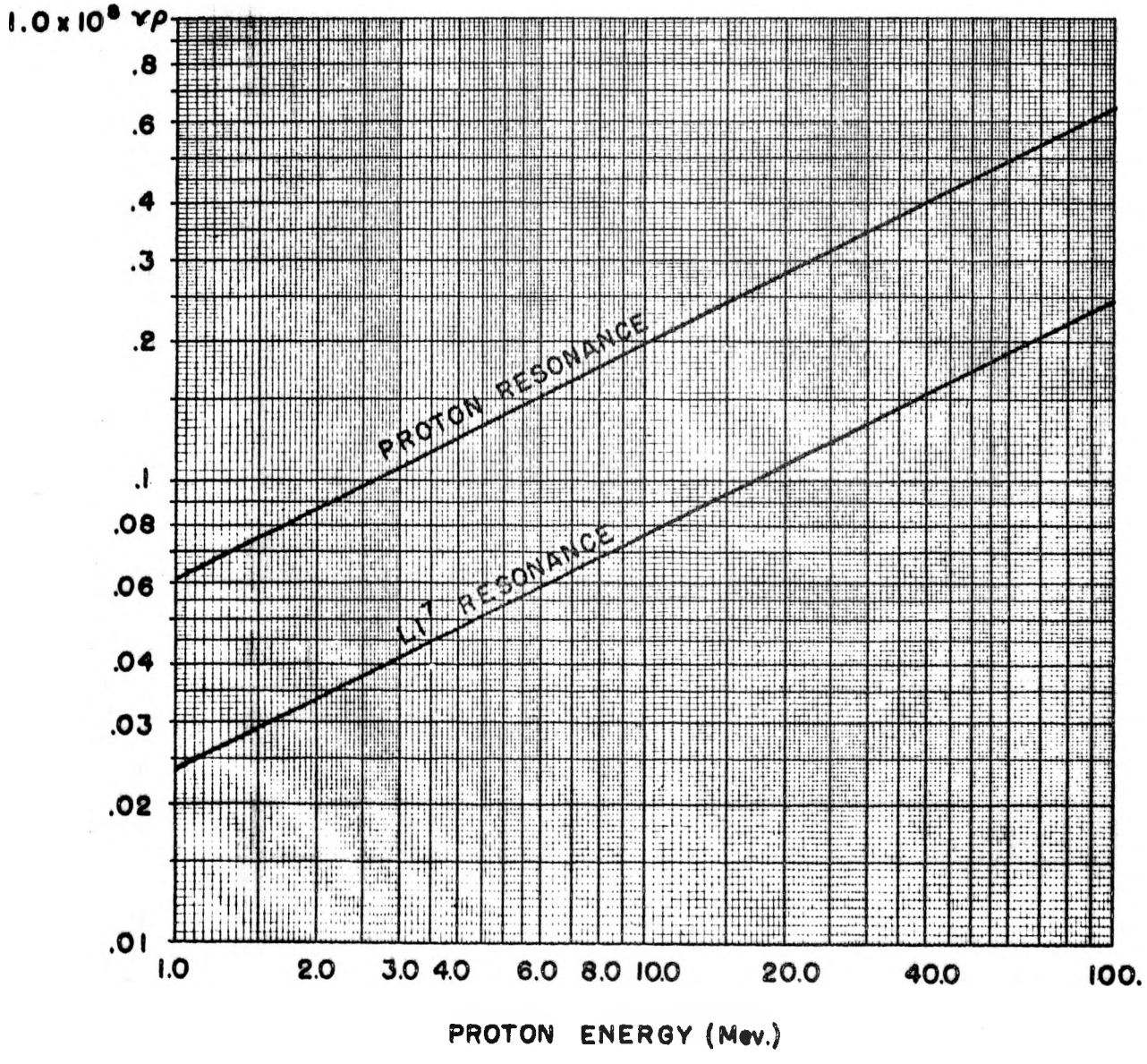

Fig. 6. $\nu\rho$ vs. E_p graph. This graph permits to determine the proton or Li^7 N M R frequency (hence the magnetic field) which will place protons of a given energy E_p at any designed position x along the image surface.

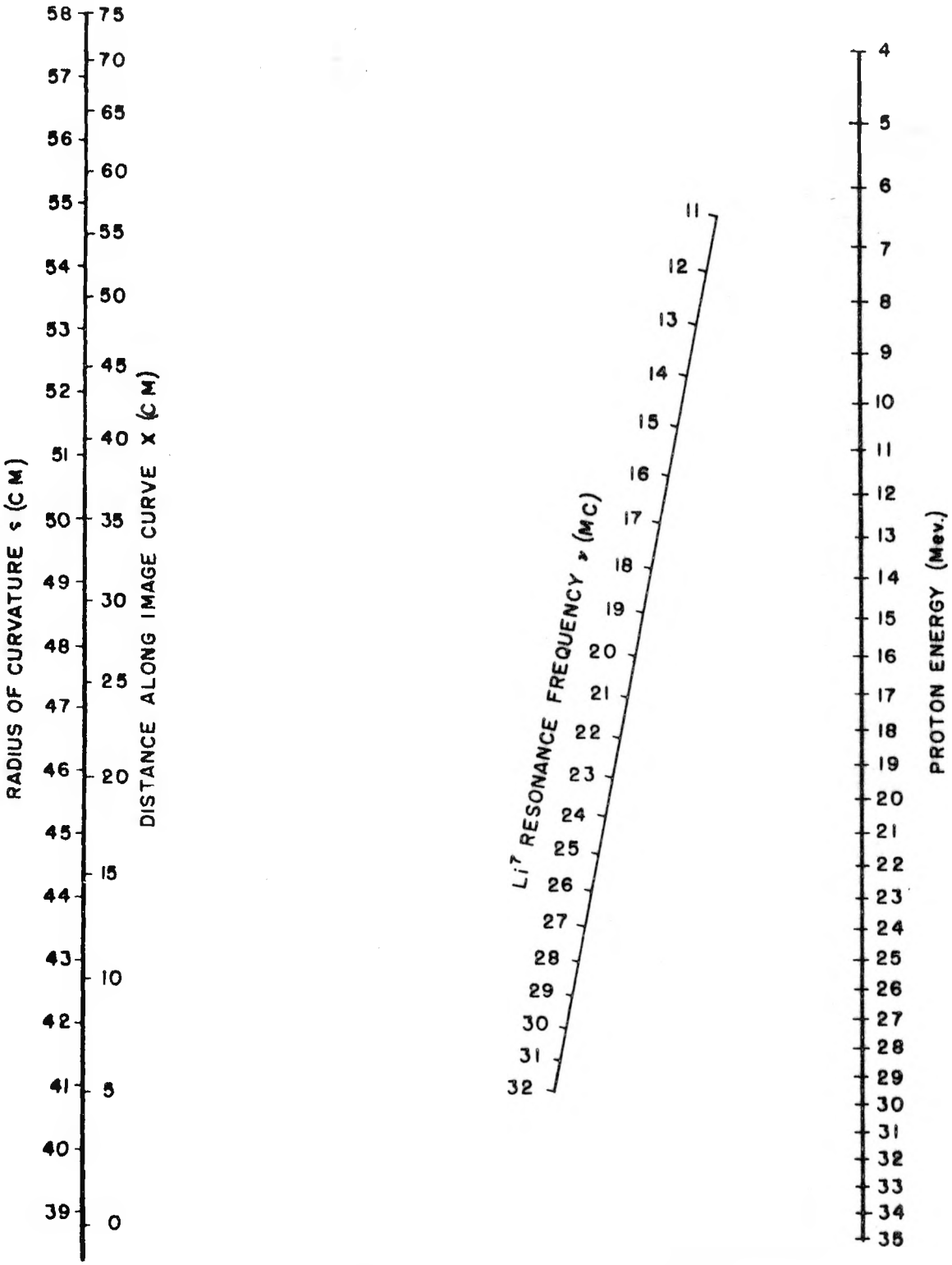

Fig. 7. Spectrograph nomogram permitting direct determination of the field setting to place protons of energy E at any desired image position X. Similar nomograms have been constructed for deuterons, He^3 and alphas.

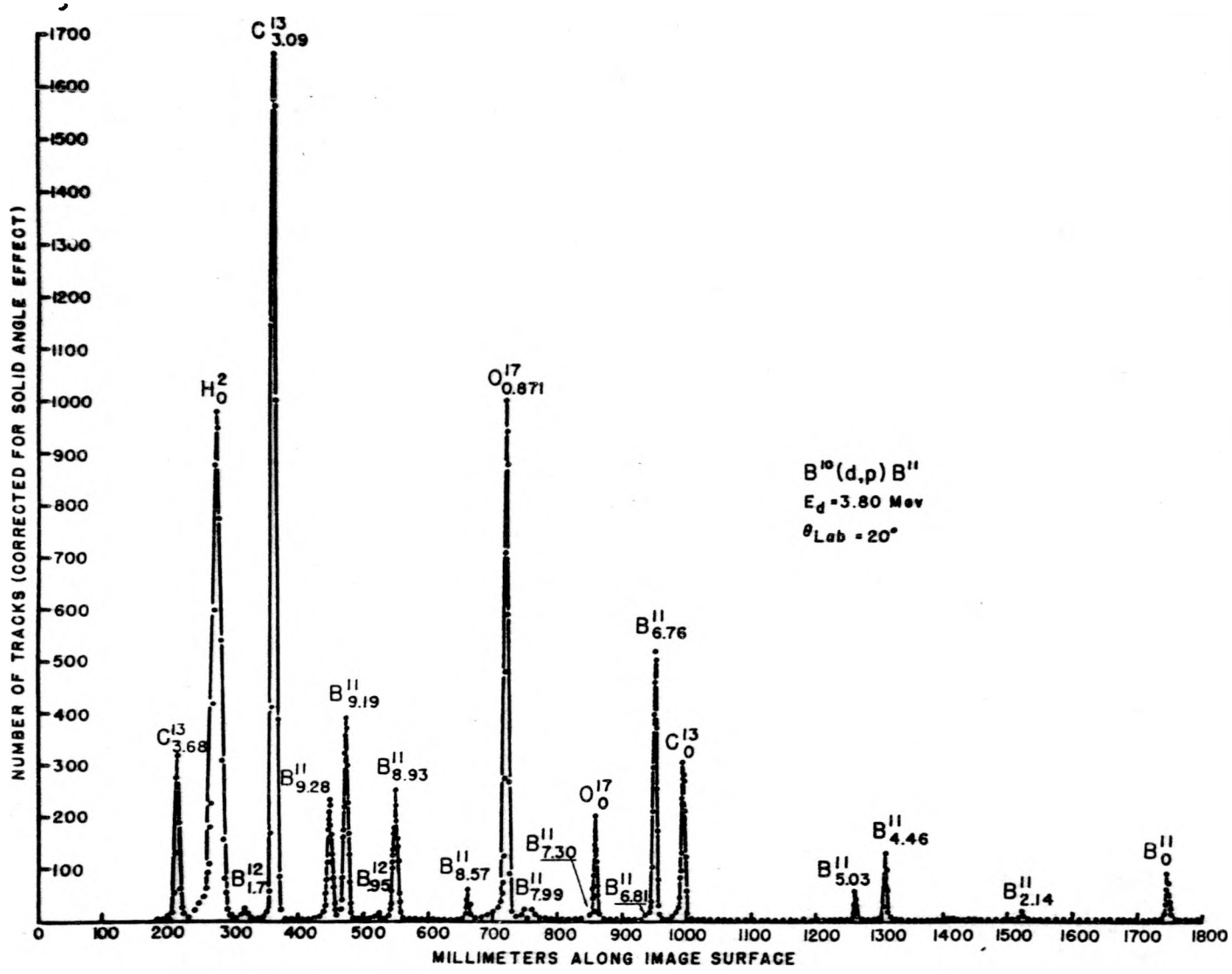

Fig. 8 Proton spectrum from the $B^{10}(d,p)B^{11}$ reaction recorded in nuclear emulsions on the image surface of the Rochester spectrograph. This spectrum represents three overlapping exposures. Peaks are corrected for the solid angle effect so that their relative sizes reflect the relative differential cross sections.

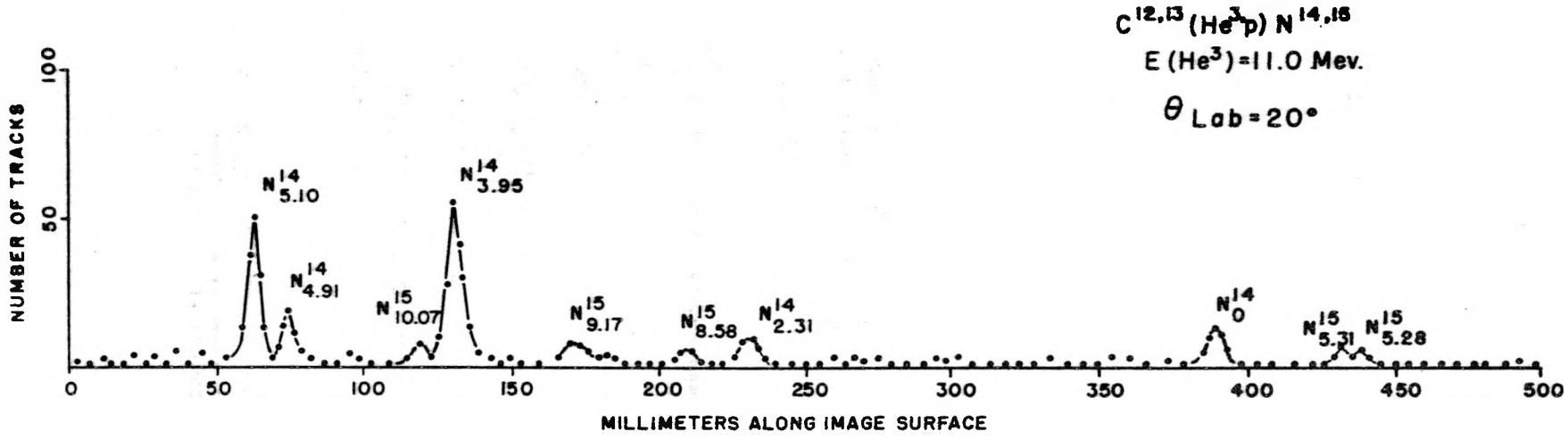

Fig.9 Spectrum of $C^{12}(He^3,p)N^{14}$ and $C^{13}(He^3,p)N^{15}$ obtained in a single exposure of nuclear emulsions in a test of a self-supporting carbon target enriched in C^{13}. It may be noted that the doublet $N^{15}(5.31)$-$N^{15}(5.28)$ which is separated by only 30 kev is partially resolved. The beam spread and target thickness are responsible for most of the width of the peaks.

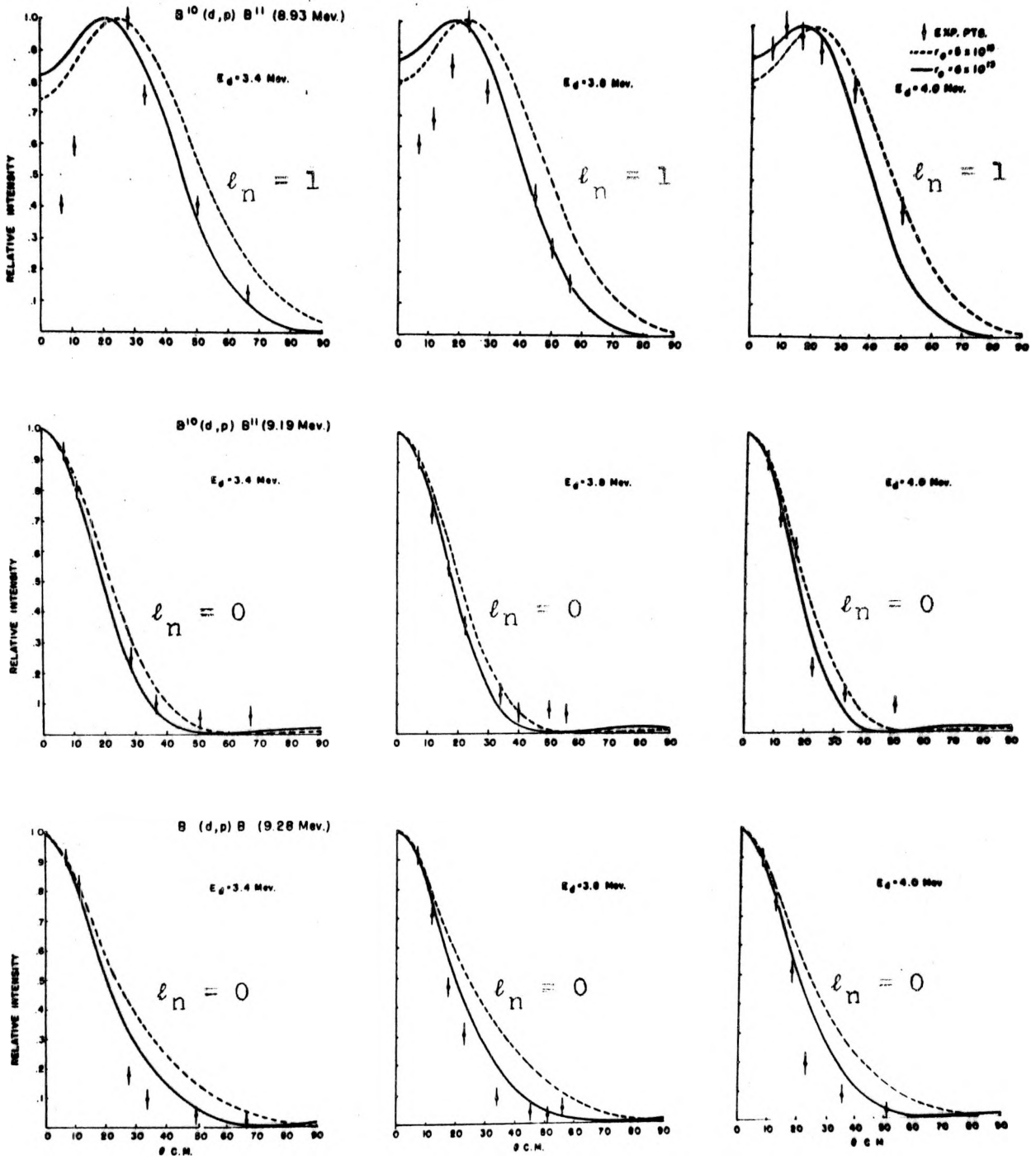

Fig.10 $B^{10}(d,p)B^{11}$ angular distributions at bombarding deuteron energies of 3.4 Mev, 3.8 Mev and 4.0 Mev, leading to the 8.93 Mev, 9.19 Mev and 9.28 Mev excited states of B^{11}. While $\ell_n = 0$, and hence even parity are again clearly confirmed for the 9.19-9.28 Mev doublet, the 8.93 Mev state is well fitted with $\ell_n = 1$ curves.